Chapter

Applications of MEMS Gyroscope for Human Gait Analysis

Hongyu Zhao, Sen Qiu, Zhelong Wang, Ning Yang, Jie Li and Jianjun Wang

Abstract

After decades of development, quantitative instruments for human gait analysis have become an important tool for revealing underlying pathologies manifested by gait abnormalities. However, the gold standard instruments (e.g., optical motion capture systems) are commonly expensive and complex while needing expert operation and maintenance and thereby be limited to a small number of specialized gait laboratories. Therefore, in current clinical settings, gait analysis still mainly relies on visual observation and assessment. Due to recent developments in microelectromechanical systems (MEMS) technology, the cost and size of gyroscopes are decreasing, while the accuracy is being improved, which provides an effective way for qualifying gait features. This chapter aims to give a close examination of human gait patterns (normal and abnormal) using gyroscope-based wearable technology. Both healthy subjects and hemiparesis patients participated in the experiment, and experimental results show that foot-mounted gyroscopes could assess gait abnormalities in both temporal and spatial domains. Gait analysis systems constructed of wearable gyroscopes can be more easily used in both clinical and home environments than their gold standard counterparts, which have few requirements for operation, maintenance, and working environment, thereby suggesting a promising future for gait analysis.

Keywords: inertial sensors, inertial measurement units (IMU), gait detection, gait features, gait abnormalities, gait disorders, wearable sensors, body sensor networks (BNS), medical applications

1. Introduction

Gait analysis is the analysis of various aspects of the patterns when we walk or run, which are the most common forms of human legged locomotion, as shown in **Figure 1**. Normal gait is achieved when the multiple body systems function properly and harmoniously, including visual, vestibular, proprioceptive, musculoskeletal, cardiopulmonary, nervous systems, etc. Injury or disease of any system may result in abnormal gait with symptoms and dysfunction of joints and muscles [3–5]. Therefore, gait performance is considered to be an indicator and predictor of overall health and functional status of individuals [6–8]. Gait analysis is an active research area for many medical, clinical, and healthcare applications. The validity and reliability of gait analysis depend strongly on the used measuring instruments. Generally, high-quality gait analysis requires accurate, detailed, and comprehensive spatiotemporal characterization of the actual locomotion pattern.

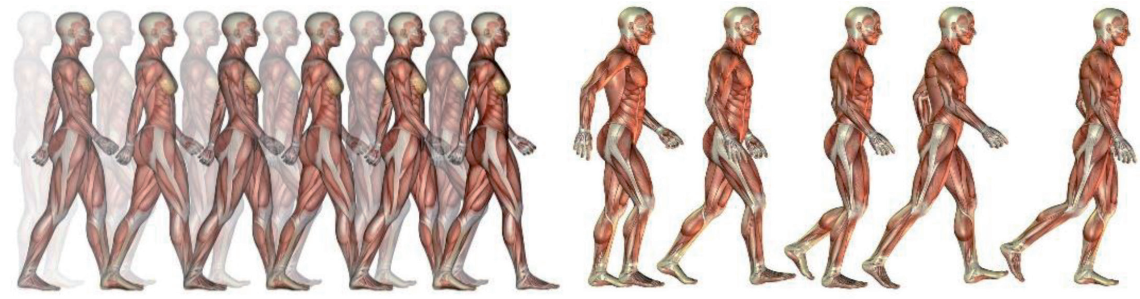

(a) (b)

Figure 1.
Human gait. (a) Walking gait [1] and (b) Running gait [2].

(a) (b) (c)

Figure 2.
Commonly used gait analysis methods. (a) Visual gait analysis [9], (b) Vicon systems [10], and (c) BTS GAITLAB [1].

At present, gait analysis in most clinics and health centers is still mainly achieved by patient self-reporting and clinician (physician, nurse, etc.) observation, as shown in **Figure 2(a)**. These subjective and qualitative methods are only suitable for preliminary gait examination. Although some severe gait abnormalities can be visually observed by human eyes, subtle differences might be overlooked without quantitative measurements [11]. With the aid of simple tools like measuring tape, stopwatch, and goniometers, as well as methods allowing leaving footprints on the ground, basic quantitative measures can be derived, such as the number of walked strides/steps, gait cadence, gait speed, stride/step length, stride time, and distance covered. The advantages of the visual observation method and foot-printing method lie in several aspects: (1) they do not require any expensive measuring instruments and complex preparation procedures; (2) they have no special requirements for the working environment; and (3) they can achieve a preliminary gait analysis in a very short time. However, the obtained measures are too limited to assess human gait, as gait is complex and multifactorial in terms of its control mechanisms governed by the neuromuscular system. Besides, the quality of measures is dependent on the observer's experience and the patient's tolerance, especially the inter- and intra-observer variability, which has been shown to significantly influence the disease-specific severity assessment and the subsequent treatment planning.

To provide high-quality quantitative information and objective measurements (some of which might not be measurable with normal clinical examinations) needed for gait analysis, gold standard gait analysis tools have been applied in some specialized centers and clinics, such as optical motion capture systems and force plates. The commonly used such systems are illustrated in **Figure 2(b)** and **(c)**, where the optoelectronic systems capture spatial gait information with infrared cameras tracking the body movement (defined by reflective markers placed on the body), while the force plates provide dynamic gait information by the measuring ground reaction forces (GRFs) based on inverse dynamics. When synchronized with each other, these systems can provide both kinematic and dynamic gait information during walking and running. However, although such systems can achieve high-precision gait analysis, they also have many drawbacks, such as their relatively high cost, long setup time, and complicated operation. Furthermore, they are confined to the restricted area where the systems are deployed and hence affect normal movement of the subjects, which may make the derived information fail to reflect the gait patterns in real-world settings. Generally, people only show their natural gait when they are accustomed to the walking environments.

Electromyography (EMG) systems are another quantitative gait analysis technology commonly used in gait-related applications. Such systems can record the electrical signals generated by skeletal muscles and hence provide insights into the patterns of muscle recruitment and neuromuscular control during walking. They are particularly suitable for investigating gait abnormalities manifested by muscle weakness and spasticity. However, EMG measuring is inconvenient in daily usage, as it requires gel, skin treatment, or smart clothes with embedded textile electrodes, especially for the traditional EMG systems that have intricate wires connecting the electrodes and the signal processor.

For gait analysis, accuracy is not always the only or primary concern, and other relevant concerns include simplicity, accessibility, portability, etc. For example, it might be more meaningful to monitor gait patterns for patients or elders in their daily lives than just a brief examination in a clinic or a gait lab [12]. Therefore, although the optoelectronic, force platform, and EMG systems have been applied to gait analysis in the past decades, they are not pervasive enough, even in specialized centers and clinics, which makes the potential of gait analysis not been fully exploited thus far. In order to make gait analysis more accessible and usable, the use of alternative instruments has been investigated to address the limitations of the gold standard methods, such as inclinometers, goniometers, air pressure sensors, foot switches (or force-sensitive resistors), and inertial sensors. These instruments are more portable, convenient, cost-effective, and easy-to-use, among which inertial sensors are widely considered attractive alternatives. Recent advancements in microelectromechanical systems (MEMS) technology paved a way to develop wearable gait analysis systems constructed of inertial measurement units (IMUs), which have shown remarkable progress in the last two decades. MEMS inertial sensors include gyroscope, accelerometer, as well as a combination of gyroscope, accelerometer, and magnetometer [13, 14]. The commonly used MEMS IMUs in the literature are shown in **Figure 3**.

Notable use of inertial sensors in gait analysis is in providing rich kinematic information about the movement patterns of different body segments. However, there are issues related to the accuracy of the measurements from these low-cost

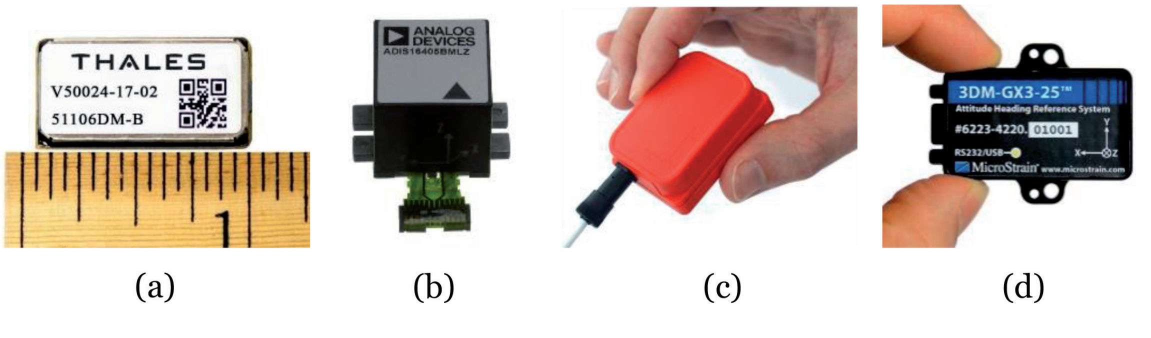

(a) (b) (c) (d)

Figure 3.
Commonly used inertial sensors based on MEMS technology. (a) InterSense IMU, (b) ADI IMU, (c) Xsens IMU, and (d) MicroStrain IMU.

MEMS sensors. The derived angle and position estimates are usually corrupted by varying sensor noises and biases, thereby resulting in the well-known continuously increasing error called drift, i.e., angular or positional deviations away from the ground truth. Many researchers addressed these issues and presented different methods to improve the system accuracy. It should be noted that the costs of MEMS accelerometers are decreasing while the accuracy is being improved, whereas the MEMS low-cost gyroscopes could not achieve the required accuracy for precise long-term positioning applications. Generally, MEMS gyroscopes have large bias drifts that can accumulate several degrees of orientation error during even 1 min. Such large error rates make it difficult to choose reasonably priced gyroscopes for inertial navigation applications, and hence the reliability and accuracy of gyroscopes are questionable [15, 16]. However, for gait analysis applications, gyroscope is the preferred device among the inertial sensors, due to the effects of human locomotion that rotational motion is more pronounced than translational motion. The systems using solely gyroscopes can provide both temporal and spatial gait parameters, whereas most other systems using accelerometers or foot switches are limited to temporal parameters merely. Therefore, the purpose of this chapter is to demonstrate the applications of MEMS gyroscope for human gait analysis.

2. Gait characterization

Generally, pathological gait shows a characteristic pattern with abnormal speed and range of joint movements, such as shortened stance phase, reduced gait cadence, limited extension/flexion, or inversion/eversion ankle movements. Professional physicians could easily recognize gait abnormalities and visually evaluate patients' progress during the physiotherapy treatments; however, quantitative measures allow a detailed description of these abnormalities, which would be desirable for diagnostic and therapeutic use. In this section, the system setup and ankle angles are first described, then the typical modes of dividing a gait cycle are discussed, and finally step lengths that can be provided by foot-mounted gyroscopes are discussed.

2.1 Ankle angles

In biomechanical analysis, kinematic information is a well-established set of gait parameters. To estimate spatiotemporal parameters, wearable gait analysis systems have been discussed in the literature, with two, three, four, or more gyroscopes attached to subject's lower limbs, such as the foot, shank, or thigh. Accurate orientation estimation using gyroscopes has been a major research interest in this field. For wearable systems, a reduction in the number of sensing units is highly desirable, as the system will be more portable, convenient, reliable, cost-effective, and easy-to-use, due to the reduction of total cost and weight, the power consumption and memory requirement, the time and operation needed for system setup, the hindrance to natural movement, etc.

For most types of pedal locomotion achieved by legged motion of human or animals, the intuitive experience is to implement gait analysis by attaching sensors to the feet. As the foot is the part of the lower limb distal to the leg, it functions as the interface between the lower limb and the ground and withstands high static and dynamic stresses that generate strong compression and shearing forces, making the periodic nature and disease symptoms of the foot more obvious than that of other parts of the lower limb. For example, diabetic foot is the distal ankle involvement induced by various causes, mainly because of the interaction of peripheral

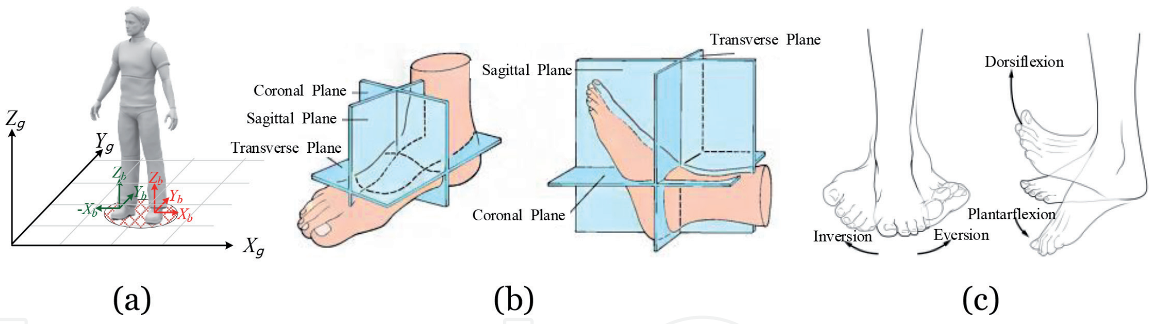

Figure 4.
Dual-sensor configuration for gait analysis and associated ankle angles. (a) Coordinate systems, (b) Foot anatomical planes and (c) Ankle movements.

vasculopathy, neuropathy, and alterations in foot biodynamics [17]. Therefore, the foot is a preferred location of gyroscopes for gait data collection.

A dual-sensor configuration with one sensor on each foot is discussed in this chapter, as illustrated in **Figure 4(a)**, which is supposed to be a promising way for wearable gait analysis. As is seen, two coordinate frames are introduced for gait analysis purpose, which are defined as follows.

- The body coordinate frame (b-frame for short) is parallel to the sensor's axes.
- The global coordinate frame (g-frame for short) is a local east-north-up (ENU) reference frame.

Such system can yield the angles of ankle movements, such as plantarflexion and dorsiflexion movements in the sagittal plane, as well as the inversion and eversion movements in the coronal plane, as shown in **Figure 4(b)** and **(c)**. These movements are described in terms of Euler angles to assess the ankle joint, as ankle rehabilitation includes range of motion training on eversion and inversion as well as plantarflexion and dorsiflexion.

2.2 Gait phases

To analyze gait abnormalities, temporal gait parameters should be estimated first. Terminologically, gait is the movement pattern involved during locomotion, which exhibits periodic patterns termed as gait cycle. Each gait cycle is characterized by a sequence of ordered gait events that occur at specific temporal locations. These events can be detected by using the measurements of wearable MEMS gyroscope. Different researchers pay attention to different gait events according to their specific application requirements. Normally, there are four typical events in one gait cycle, i.e., heel-strike (HS), foot-flat (FF), heel-off (HO), and toe-off (TO), as shown in **Figure 5** identified relative to the right foot and defined in the following way:

1. **HS event**: the heel strikes the ground.
2. **FF event**: the toe touches the ground, and the foot becomes completely flat on the ground.
3. **HO event**: the heel leaves the ground.
4. **TO event**: the toe leaves the ground, and the foot becomes totally in the air.

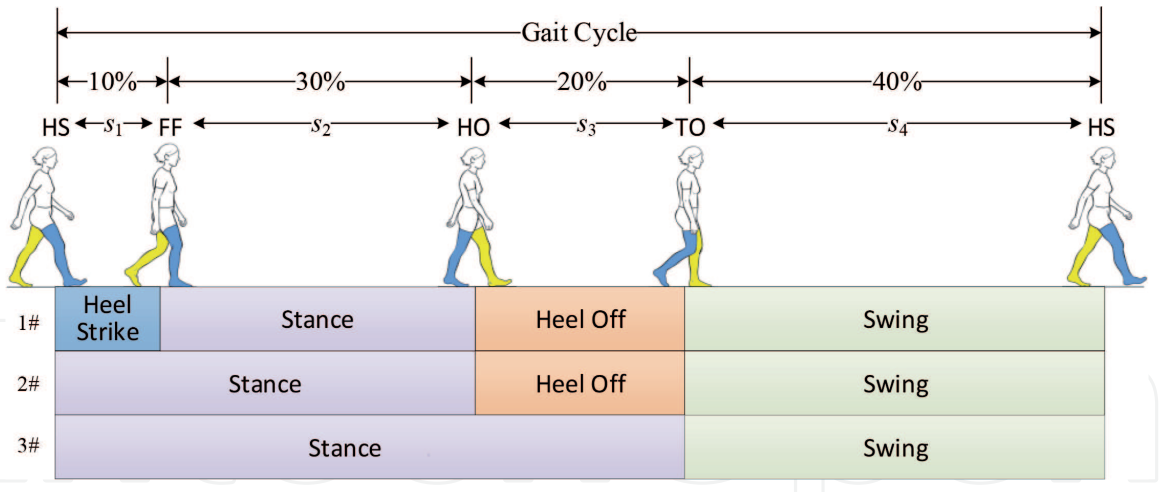

Figure 5.
Typical events and phases in one gait cycle.

Usually, HS event is specified as the beginning of a gait cycle, and a complete gait cycle is defined as the time interval between successive HS events of the same foot. The typical gait events can divide a gait cycle into two to four consecutive time intervals termed as gait phases. When considering more gait events, e.g., mid-stance and mid-swing, more gait phases will be delimited, which is not addressed in this chapter. As shown in **Figure 5**, there are three common modes of gait cycle division. The first mode (1) divides a gait cycle into two phases, i.e., stance and swing, where the stance phase lasts from HS to TO corresponding to about 60% of a gait cycle [18]. The second mode (2) divides a gait cycle into three phases, where the stance phase is delimited by HS and HO constituting about 40% of a gait cycle [19]. The third mode (3) divides a gait cycle into four phases, where the stance phase lasts from FF to HO comprising about 30% of a gait cycle [20].

Obviously, out-of-sequence events are not permitted in normal gait, and hence a breakdown in gait rhythm and bilateral coordination plays a significant role in identifying pathologic gait, e.g., freezing of gait in Parkinson's disease. Besides, for the patients with gait abnormalities, the affected lower limb fails to support the body weight well, which makes the corresponding stance phase short-lasting and results in a highly unstable situation. Monitoring gait cycle distribution in temporal domain has been applied to detect the onset of neurodegenerative diseases and injuries [21].

In this chapter, for demonstration purpose, the mentioned four typical gait events are modeled and identified, and hence a normalized gait cycle is divided into four phases as that in the first division mode (1). In this division, the stance phase is the time interval when the foot is entirely on the ground, the swing phase is the time interval when the foot is entirely in the air, and the two remaining phases are the transition states between stance and swing. Furthermore, as the motions of subject's two feet are strongly coupled with each other, detecting gait events using the measurements of both feet is supposed to obtain more accurate results than just using that of the ipsilateral limb. When the concerned gait events of each foot are correctly detected, the gait cycles will be divided, the gait phases will be delimited, and therefore the temporal gait parameters will be derived accordingly.

2.3 Step lengths

When the gait phases are delimited, the spatial gait parameters can be derived accordingly. The distance-related gait parameters involve step length, step width, and step height, corresponding to the maximum covered distance in the forward, lateral, and vertical directions, respectively, over a step, as shown in **Figure 6**. Among these

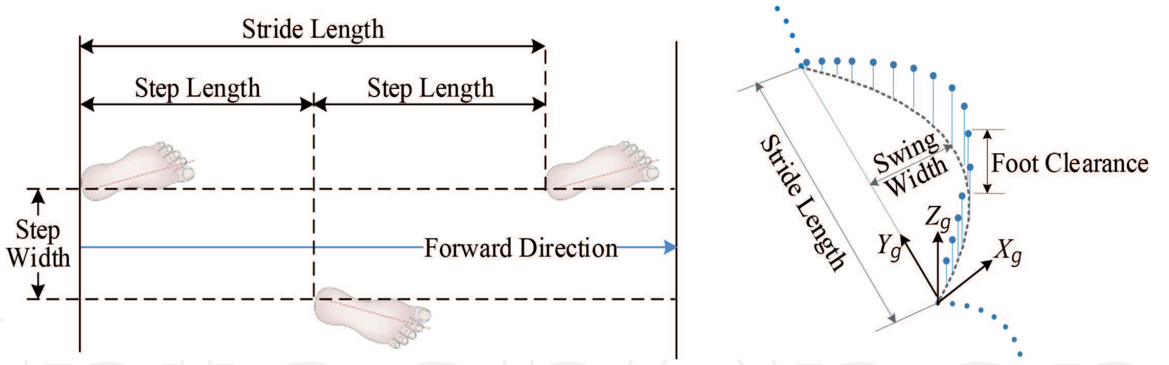

Figure 6.
Distance-related spatial gait parameters.

three parameters, the step length in the sagittal plane needs to be calculated separately for each step of each individual, as it varies considerably due to inter- and intraindividual gait variability. Actually, several factors can account for the phenomenon of gait variability, such as leg length, walking speed, and gait pattern. Step length has different values among the literature data. As reported in [22], the average step length is around 0.75 m for healthy adults walking at their self-selected normal speed of about 1.4 m/s, while, as reported in [23], the average step length varies with gender, which is about 0.79 m for males and 0.66 m for females.

As shown in **Figure 6**, a stride consists of two consecutive steps. Both stride length and step length are meaningful gait parameters to assess gait performance. Gait slowness with reduced step length is a manifestation of diseases affecting walking ability, such as spinal cord injury, stroke, Parkinson's disease, and osteoarticular disorders. Many methods for estimating step length and gait speed have been proposed in the literature, e.g., using a mathematical model. Prior studies have employed a single inverted pendulum model to estimate the step length [24], by using a uniaxial gyroscope. A more sophisticated method presented in [25] employs a double pendulum model comprised of an inverted double pendulum pivoting about the ground during stance and a double pendulum pivoting about the hip during swing. A four-sensor configuration is proposed to deal with the non-pendulum nature of double limb support [26]. Typically, a gait model can be driven by various combinations of direct or indirect gyroscope measurements, with the sensors attached to the subject's shank, thigh, or lower lumbar spine near the body's center of mass (COM), etc. Comparisons between different step length estimators are presented in [27].

Based on different gait models, necessary relations between the step length and various measurable or computable gait variables can be formulated. For the dual-sensor configuration shown in **Figure 4(a)**, a modified gait model was presented in our previous study [28], which is driven by the measurements from foot-mounted gyroscopes solely. In this model, human gait is represented by a single inverted pendulum model of a kneeless biped, taking the anthropometric data specific to each subject's biomechanics into consideration, as shown in **Figure 7**. This model functions as a self-contained step length estimator, which does not simply resort to other ranging technologies based on infrared, RF, or ultrasonic devices that usually use some type of beacon or active badge [29, 30] nor directly double integrate the gravity-compensated translational acceleration over time. The step length S_L can be estimated as the forward distance traversed by the body's COM, during the stance phase of the contralateral rear foot that supports the forward motion of the swing leg.

Therefore, a mathematical model from indirect gyroscope measurements can be adopted to estimate the step length by

$$S_L = L \cdot [\sin(\theta_1) + \sin(\theta_2)] \tag{1}$$

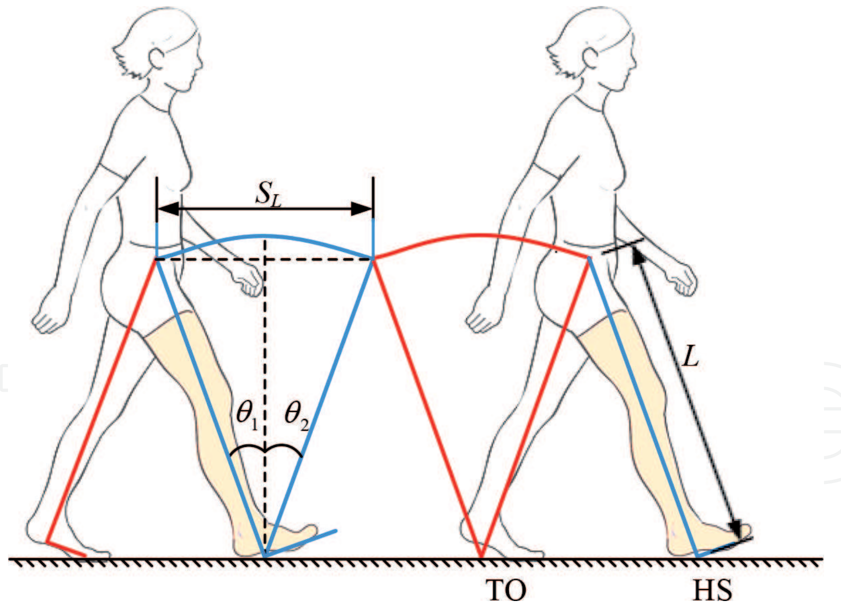

Figure 7.
Kneeless inverted pendulum model of walking gait.

where L denotes the pendulum length related to the subject's height and leg length and θ_1 and θ_2 denote the amplitudes that the pendulum swings away from vertical, which are approximated by the maximum positive and negative rotation angles of foot pitch motion, respectively, and related to the plantarflexion and dorsiflexion angles on the sagittal plane.

3. Gait data acquisition

Gait analysis can be achieved by examining the patterns of sensed data from the measuring instruments. There are two sources of gait data in our study, i.e., inertial data and optoelectronic data. The optoelectronic data are measured by using the Vicon® optical motion capture system from Oxford Metrics Ltd., UK [10], which is used as reference data to provide ground truth for gait analysis algorithms. As illustrated in **Figure 8(a)**, the MEMS inertial sensors and Vicon retroreflective markers are attached to the subject's lower limbs. However, for demonstration purpose, only the measurements from foot-mounted devices are considered in this chapter, as shown in the partial enlarged drawing in **Figure 8(b)**. Two types of inertial

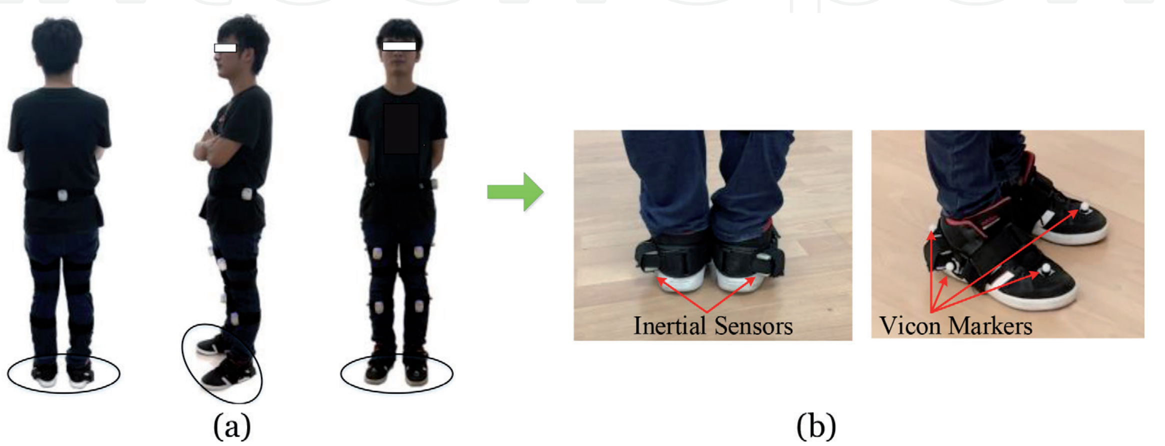

Figure 8.
System setup for gait data acquisition. (a) Sensor placement on lower limbs and (b) Foot-mounted sensors and markers.

sensors are used for gait data collection in our study, i.e., Nano IMU (nIMU) from MEMSense Inc., USA [31], and ADIS16448 *i*Sensor® device from Analog Devices Inc., USA [32], as described below.

3.1 MEMSense IMU

The first type of inertial sensors used in our study is the MEMSense nIMU [13, 33], which is a small-size and low-weight MEMS unit and costs about $1300, as shown in **Figure 9** that illustrates the data acquisition process under normal conditions. Since nIMU is a wired sensor node, when communicating with it, one needs to connect it to a USB interface board first and then connect the USB interface board to a computer for further processing. The software used for acquiring and storing sensed data is the MEMSense IMU Data Console (IDC), which is a console-based, menu-driven application and allows basic display and collection using a specified RS422 protocol.

The nIMU is compensated for temperature sensitivities to bias and scale factor and provides serial outputs including 3D acceleration, 3D angular rate, and 3D magnetic field intensity, with a sampling rate of 150 Hz. The key manufacturer specifications of the gyroscope in nIMU are listed in **Table 1**.

A segment of raw measurements is shown in **Figure 10**. As the IMUs are placed on the subject's feet, the gyroscope measurements feature periodic and repetitive patterns according to the transitions of gait phases. These patterns are helpful for gait analysis, by facilitating the detection of the key gait events and the concerned gait phases correspondingly. Since the feet are exposed to quite extreme dynamics at HS events, it is found that the bandwidth and dynamic ranges of the gyroscope in nIMU are insufficient for optimal gait characterization, as seen in **Figure 10**. These insufficiencies would induce systematic measurement and modeling errors to the system. When testing the sensor for running gait, the achieved tracking results are reasonable but would improve considerably if the gyroscope has sufficient dynamic range, so as to accurately monitor the impact of foot on the ground. According to research in [34], the maximum angular velocity experienced by toe-mounted gyroscopes can

Figure 9.
MEMSense nIMU used for gait data collection.

Mass (g)		20
Size (mm)		45 × 23 × 13
Operating temperature (°C)		0 to +70
Gyroscope	Range (°/s)	±600
	Nonlinearity (% of FS)	±0.1
	Noise (°/s)	0.56 (0.95)
	Bandwidth (Hz)	50

Table 1.
Key specifications of gyroscope in MEMSense nIMU.

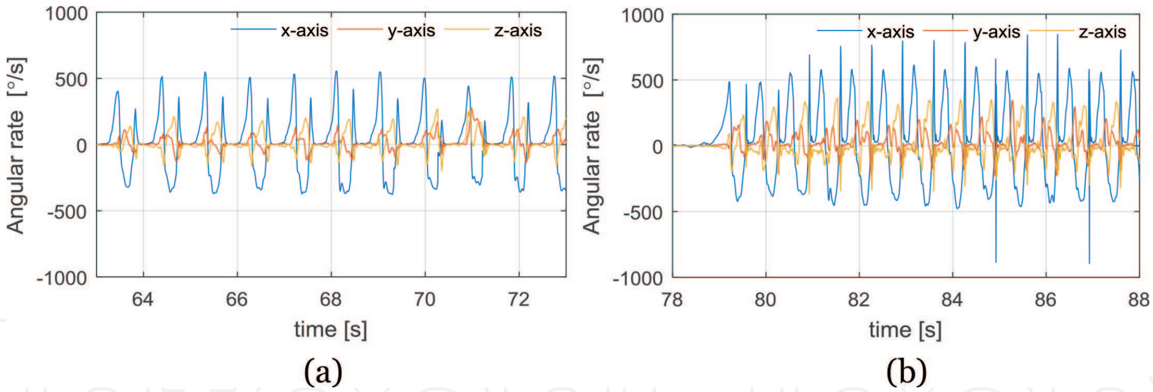

Figure 10.
Raw gyroscope measurements of MEMSense nIMU. (a) Walking at 130 steps/min anf (b) Running at 170 steps/min.

reach 1500°/s during running and 2000°/s during sprinting. This is because the foot attitude changes very rapidly over the gait cycle, especially for the toe motion that exhibits the highest angular velocity. The maximum angular velocities experienced by the heel, ankle, and shin are no higher than 1000°/s during running.

3.2 Analog devices IMU

The other type of inertial sensors used in our study is the ADIS16448 *i*Sensor® device [35–37], which combines industry-leading *i*MEMS® technology with signal conditioning that optimizes dynamic performance and costs about $600. The ADIS16448 is packaged in a module that has a standard connector interface, as illustrated in **Figure 11** that depicts the data acquisition process in a physical therapy and rehabilitation department of a public hospital. The SPI and register structures provide a simple interface for data collection and configuration control. The ADIS16448 has a compatible pinout for systems that currently use other Analog Devices, Inc., IMU products. Each ADIS16448 includes a triaxial gyroscope, a triaxial accelerometer, a triaxial magnetometer, and pressure sensors. The factory calibration characterizes each sensor for sensitivity, bias, and alignment. Thus, each sensor has its own dynamic compensation formulas that provide accurate sensor measurements. The key manufacturer specifications of the gyroscope in ADIS16448 are listed in **Table 2**.

The dimensions of the entire sensing assembly are 4.5 × 3.5 × 2.25 cm, and the sampling rate is 400 Hz. The main components include the ADIS16448 IMU, a printed circuit assembly (PCA) with a microcontroller, a power supply, and a casing enclosing all of the components. The collected data were stored in internal memory first and then transferred to an external computer for further processing. A segment of raw measurements is shown in **Figure 12**. It can be seen that the gyroscope

Figure 11.
ADIS16448 iSensor® *device used for gait data collection.*

Mass (g)		15
Size (mm)		24.1 × 37.7 × 10.8
Operating temperature (°C)		−40 to +85
Gyroscope	Range (°/s)	±1000
	Nonlinearity (% of FS)	±0.1
	Noise (°/s)	0.27
	Bandwidth (Hz)	330

Table 2.
Key specifications of gyroscope in ADIS16448 iSensor® device.

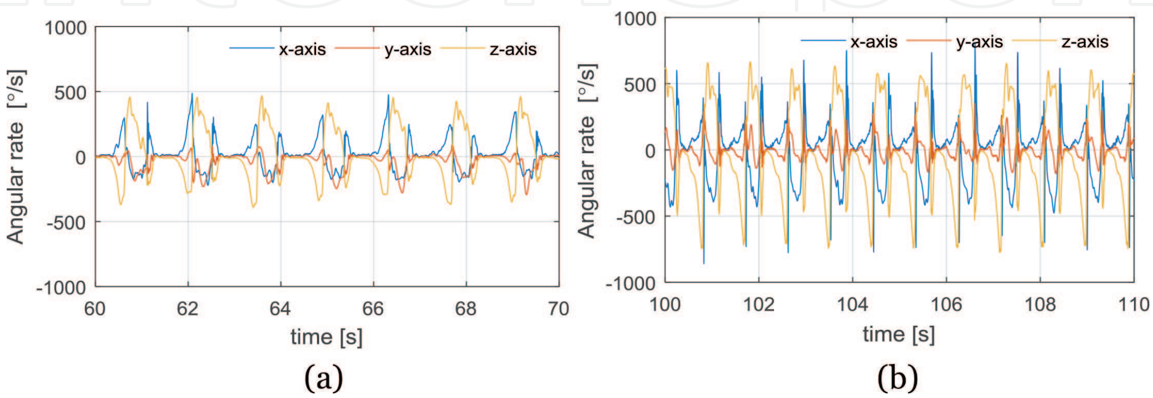

Figure 12.
Raw gyroscope measurements of ADIS16448 iSensor® device. (a) Walking at 3 km/h and (b) Running at 6 km/h.

range of ±1000°/s would be more suitable, as the sensor readings stay within this dynamic range during walking and running at varying speeds.

4. Rule-based gait detection

In this chapter, the raw measurements of accelerometer and gyroscope are compared first, then the gait events are identified by using a rule-based method, and finally the false-detected gait phases are discussed and eliminated.

4.1 Raw inertial measurements

Different methods have been presented for gait detection in the literature [38]. In a sense, gait phases are a function of time and inertial measurements. A segment of raw measurements is shown in **Figure 13**, including specific forces and angular rates of both feet measured by the accelerometer and the gyroscope, respectively, together with the key gait events and their delimited gait phases. Gait detection can be achieved by using a rule-based method from the raw measurements or its magnitude [39], root mean square [40], and moving average [41], which is straightforward and easy to implement. Different detection methods have been compared in [42], and the results suggest that angular rate is more reliable than acceleration for typical walking. As can be seen in **Figure 13**, the angular rates provide more prominent characteristics than the specific forces for gait detection, especially the angular rate around Z-axis in the sagittal plane. Due to the specificity of foot motion, there are at least two possible explanations for this phenomenon:

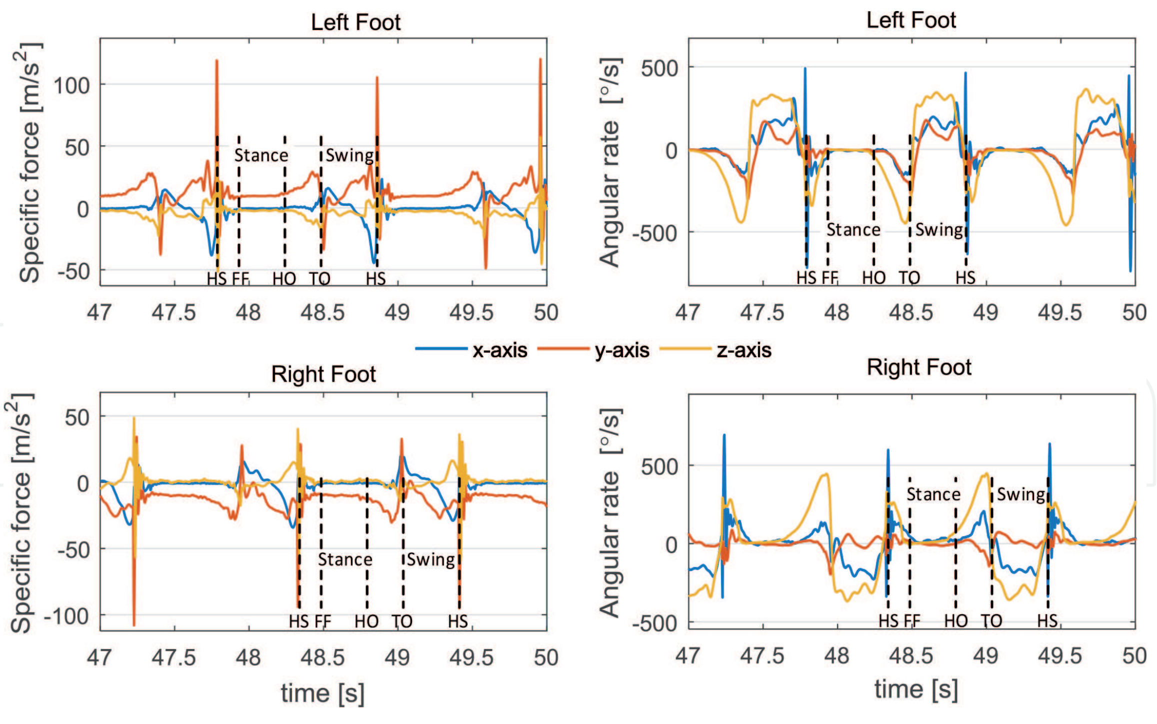

Figure 13.
A segment of raw inertial measurements from both feet.

1. Although the angular rates have large bias, their SNR (signal-to-noise ratio) is higher than that of the specific forces.

2. The specific forces are perturbed by the integrated effects of initial alignment error, gravity disturbance, and accelerometer bias.

4.2 Gait detection with predefined rules

The rules for gait detection from inertial data can be predefined against the ground truth provided by the Vicon system. Generally, three types of rules might be involved in the detection process, i.e., peak detection, flat-zone detection, and zero-crossing detection. Take the stance phase, for example, it is the nature of walking or running locomotion that the foot swings to stance phase in every gait cycle and then exhibits a zero velocity until it swings again. This information can be effectively utilized by a flat-zone detection method to identify the successive stance phases. With careful rule design and parameter selection, the rule-based methods can identify all concerned events from a long inertial data sequence.

For a straight-line walking of 20 m long, the detection results are shown in **Figure 14**. However, as seen in **Figure 13**, the measurements are characterized by some sudden spikes, especially when the HS and TO events occur, which can induce momentary fluctuations in the magnitude or short-term statistics of angular rates and thereby result in false detections of gait phases. In some research, a time heuristic method is applied to the raw detection results to avoid unnecessary influence of the measurement fluctuations, i.e., incorrectly declaring, interrupting, or missing of gait phases. This is achieved by adding a time duration threshold to filter out the gait phases that have a duration shorter than the threshold, as the false gait phases are usually short-lasting [43, 44]. However, as all the thresholds are hand-tuned, they may work well for the gait data that they are derived from, but not apply to each subject's individual gait.

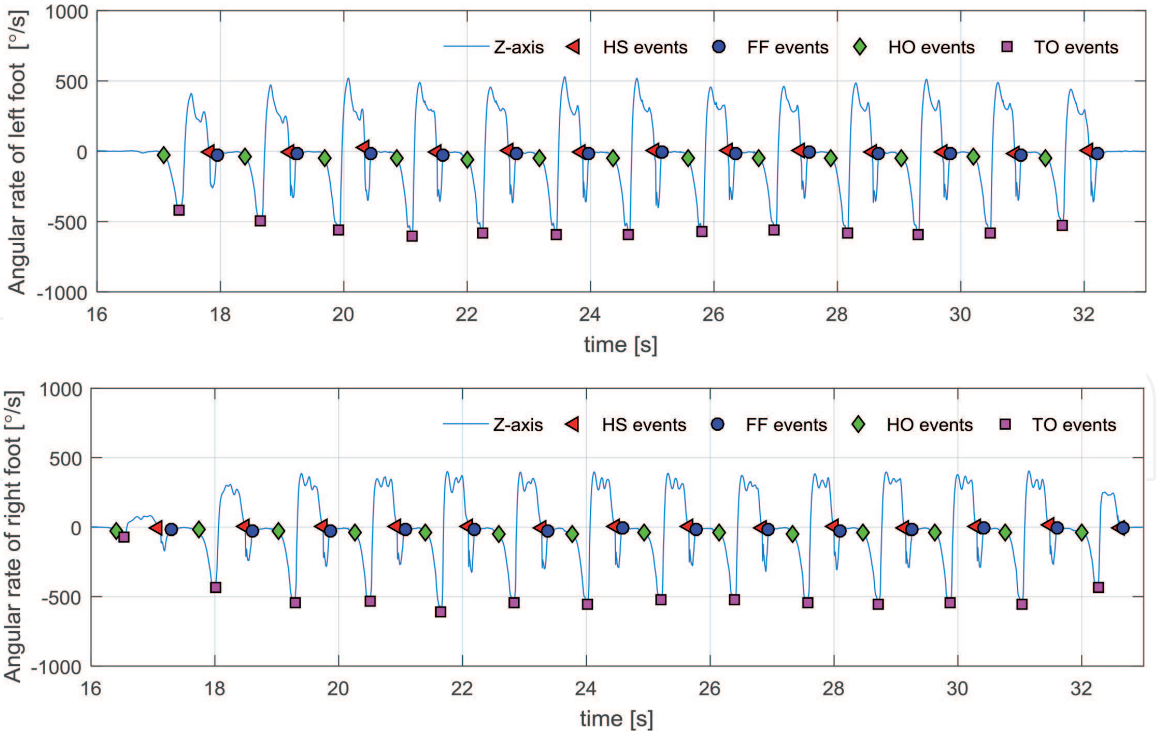

Figure 14.
Results of gait division and gait detection.

4.3 Elimination of false gait phases

As each individual has a unique gait pattern, the percentage of the gait cycle spent in each phase slightly varies between the literature sources. In literature research, it is rarely discussed explicitly how to choose a time duration threshold for eliminating the false gait phases but based on empirical evidence. Therefore, an adaptive time threshold is required to provide a more robust method for gait detection. As done in our previous study, a clustering technique can be used to automatically distinguish the true and false gait phases according to their time durations and yield the time threshold parameter simultaneously [33], as shown in **Figure 15**. In this scenario, since the number of clusters is known, the k-mean or k-median methods can be employed due to their simplicity and efficiency.

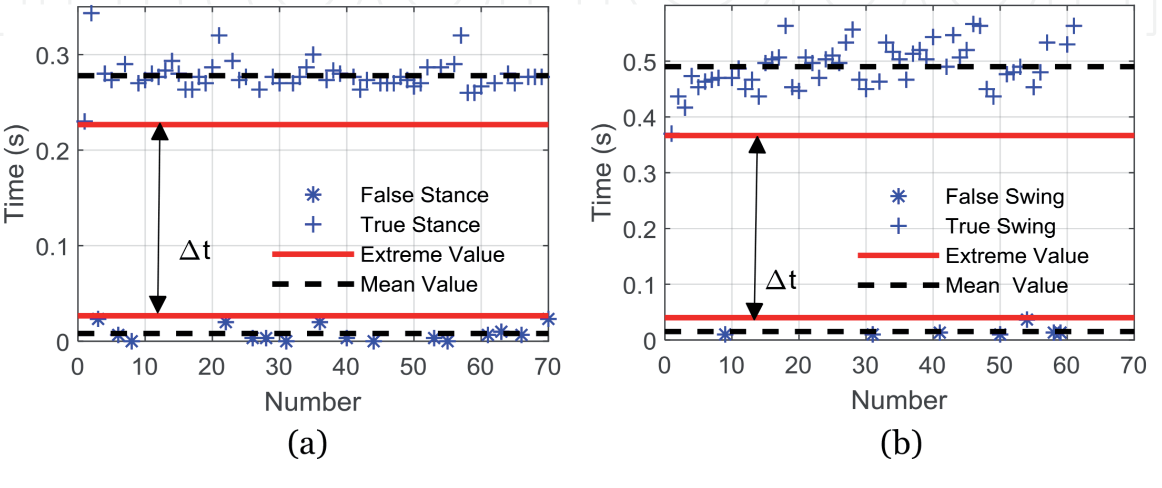

Figure 15.
Binary classification of potential gait phases. (a) Clustering of stance phases and (b) Clustering of swing phases.

Multiple parameters are involved for gait detection, which are interrelated and work together to achieve their goal. The adopted clustering technique tried to tune one of the thresholds automatically (i.e., the time threshold of gait phases) and further facilitate the choice of other thresholds, but careful parameter setting is stilled needed. Generally, rule-based methods rely on careful sensor alignment and a set of thresholds, which are brittle or difficult to implement due to the natural variability of human gait. Moreover, the thresholds are usually hand-tuned and fixed in the whole process regardless of gait changes, and the process of rule designing and threshold tuning itself is frustrating and time-consuming. Furthermore, if new sensors are added to the setup or the sensors are attached to new locations, new detection rules and associated thresholds are required. Therefore, there is a clear need of an adaptive detection method.

5. Machine learning-based gait detection

As mentioned above, gait detection is actually a pattern recognition problem. Hidden Markov models (HMMs) have been widely used for pattern recognition. An HMM-based method was developed for gait detection in children with and without hemiplegia, and the gait events were specified as hidden states [45]. A classifier based on HMM is applied for gait phase detection and discrimination between walking-jogging activities [20]. An HMM was applied to detect the gait phases of children with cerebral palsy [46]. However, HMMs are less suitable for gait data of high dimension. An HMM was adopted to estimate temporal gait parameters with a feature selection and model parametrization system based on genetic algorithms (GAs) [47]. An HMM was presented to detect gait phases with observations provided by a five-layer feed-forward neural network (FNN) [48]. Generally, these hybrid methods have better performance than the pure HMMs when dealing with high-dimensional data. Inspired by the existing methods, an adaptive hybrid method is presented in our previous study [36], by modeling human gait with a left-right HMM and employing a three-layer neural network (NN) to deal with the raw measurements.

5.1 HMM-based gait model

HMM is a statistical model used to represent discrete and stochastic Markov process, in which the states cannot be directly observed. It can be of three types, i.e., ergodic, left-right, or parallel left-right. At each time instant, HMM is in just one state. For gait detection, the gait events or their delimited phases are the hidden states of HMM. Due to the periodic nature of normal foot motion with a sequence of ordered gait events, each state can only transit to itself or the "right" state. Thus, each gait phase can be represented by a unique state in HMM using a left-right model, as shown in **Figure 16**, where a_{ij} is the state transition probability. This process yields a sequence of hidden states and a sequence of corresponding observations. Each HMM state corresponds to a gait phase that begins with the present gait event and lasts until the next event.

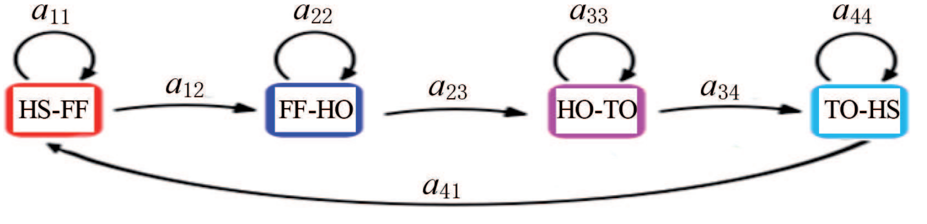

Figure 16.
Left-right HMM with four gait phases.

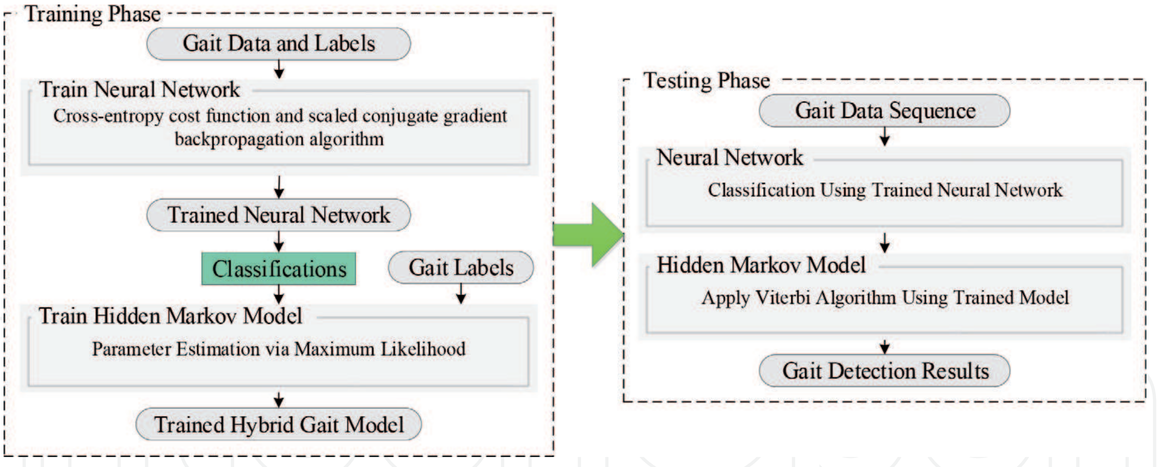

Figure 17.
Framework of the hybrid gait detection method.

5.2 NN-/HMM-based hybrid gait model

Given a sequence of ordered observations and a trained HMM, the Viterbi algorithm can estimate the most likely sequence of hidden states. However, HMMs are generative models, whereas discriminative models are supposed to achieve better classification results. Discriminative models based on machine learning techniques are perceived to be promising alternatives to HMMs [49]. Generally, any machine learning method, such as support vector machine (SVM), k-nearest neighbor (k-NN), and neural network (NN), can be used for gait detection. It is found that NNs can achieve the best trade-off between efficiency, accuracy, and computational complexity. The NNs can learn nonlinear combinations of inputs automatically, and a three-layer network can approximate any multivariate polynomial function [50]. However, the pure NNs have been limited to process inputs in isolation.

To take advantage of both NN and HMM methods for gait detection, one intuitive way is to combine them together in a hybrid manner [48]. The NN can process the gyroscope measurements first and provide observations for HMM with its classifications. Each input of NN is formed by using a sliding window approach, and hence it might be of high dimension. The HMM can model the sequential property of human gait and complement the NN by providing contextual information. **Figure 17** shows the framework of training and testing procedures of this hybrid detection method. Although the NN-/HMM-based hybrid method is computationally complex for training, it is computationally efficient at runtime. It requires no careful sensor alignment or parameter adjustment and generalizes well to new subjects, new gaits, new sensors, and new sensor locations [51].

6. Gait analysis experiment

Usually, pathological gait exhibits a characteristic gait pattern with limited range and velocity, such as shortened stance phase and step length, reduced gait cadence and gait velocity, and diminished extension-flexion movement. The outputs of wearable gait analysis system are of great use for a close examination of human gait, which allow a rapid and accurate quantification of these abnormalities. In this section, the setup and results of the experiments are first presented, then some discussions on the experimental results are made, and finally the capability of IMU-based gait analysis system for tracking the rehabilitation process is verified.

6.1 Experiment setup

Patients during the course of their rehabilitation were recruited as volunteers in our study. For comparison purpose, young healthy subjects were also recruited as volunteers to participate in the study. Prior to each trial, the subjects were asked to stand still for a few seconds to perform initial alignment of the system [52]. During each trial, the patients were instructed to walk at their comfortable speed along a straight-line path about 10 m long, which is along a hospital corridor and free of obstacles. All patients were asked to perform two consecutive walks in forward and backward directions, respectively, and return at the starting position at the end of each trial. For the healthy subjects, the experiment was performed with the same procedure, except that four consecutive walks were performed and the predefined path was 20 m long on a flat floor of a modern office building.

6.2 Experiment results

6.2.1 Single trial

When the gait events are correctly detected, the spatiotemporal gait parameters can be extracted, such as gait phase duration, gait cycle distribution, foot angle, stride length, and gait speed, as shown in **Figure 18** for a single trial.

As is seen in **Figure 18**, a gait cycle is divided into four successive phases, which are defined as follows:

- HS (HS-FF): the phase lasting from HS event to FF event
- ST (FF-HO): the stance phase
- HO (HO-TO): the phase lasting from HO event to TO event
- SW (HO-HS): the swing phase

Hemiparesis can lead to unilateral paresis, i.e., weakness of one side of the body. Compared with the normal gait of healthy subjects, several conclusions can be drawn for the pathological gait of patients from the results shown in **Figure 18**, some of which are as follows:

1. The patient exhibits a reduced gait cadence with longer gait cycle and an irregular and asymmetric gait pattern.

2. The patient is affected on the left side, as the stance phases of the left foot are shorter than that of the right side, while the opposite is true for the swing phases, which is in turn due to the affected lower limb that cannot support the body weight well alone and creates a highly unstable situation.

3. The patient exhibits a significantly diminished extension-flexion foot movement, especially for his left foot, where the shortened HS phases are manifestations of insufficient foot dorsiflexion during the swing phase.

4. The patient exhibits a shortened stride length, as although the covered distance of the patient is half that of the healthy subject, the numbers of strides taken were almost the same.

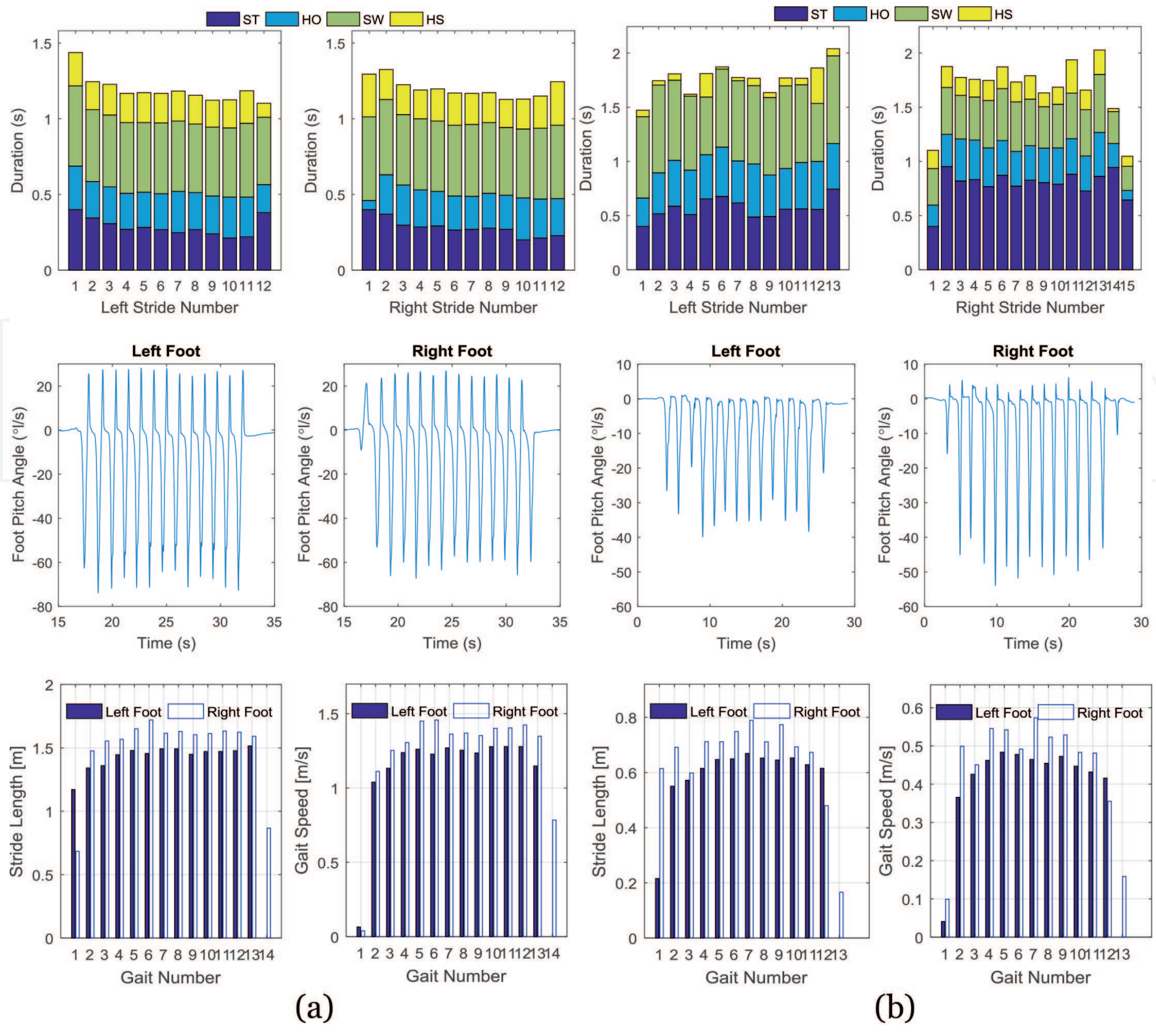

Figure 18.
Estimated spatiotemporal gait parameters. (a) Healthy subject and (b) Hemiparesis patient.

5. The patient's gait speeds of both feet are clearly reduced, and the stride lengths of both lower limbs are greatly shortened, which supports the hypothesis that the healthy side is influenced by the affected side, and the patient even has no asymptomatic side due to the so-called compensatory responses.

As discussed above, insufficient dorsiflexion of foot motion means that the patient is not capable of lifting the toe adequately during the swing phase, thereby resulting in a quick translation from swing to stance. This disorder could not only yield abnormal proportions of gait phases, affecting the gait symmetry and gait regularity, but also be dangerous to patients for being a high risk of fall as it alters the load distribution.

6.2.2 Multiple trials

More trials were performed for a rich data to increase the variability of gait patterns. For demonstration purpose, the average values and standard deviations of the durations of each gait phase and their relative percentages in each gait cycle are calculated for each concerned gait phase of all the trials, as shown in **Figures 19** and **20**. The result of multiple trials further confirms the conclusions made from that of the single trial.

6.3 Rehabilitation process evaluation

To verify the ability of IMU-based gait analysis system for evaluating the rehabilitation process, a patient's gait was measured once a week for 1 month. The

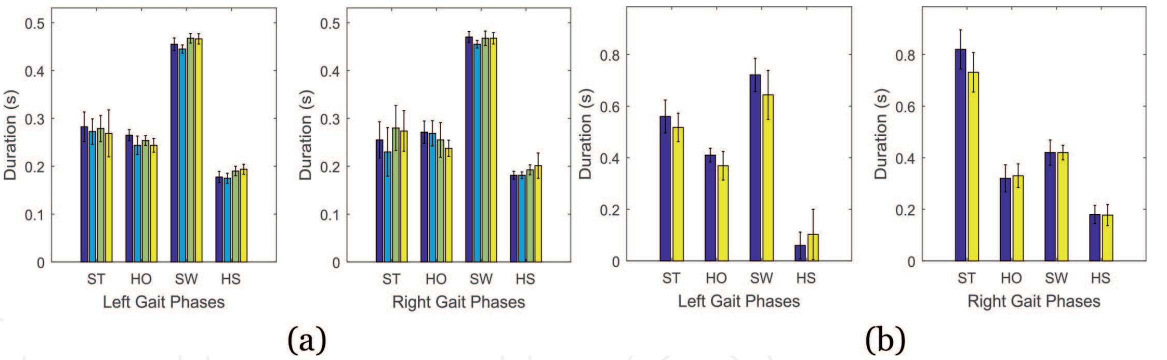

Figure 19.
Durations of the gait phases over multiple trials. (a) Healthy subject and (b) Hemiparesis patient.

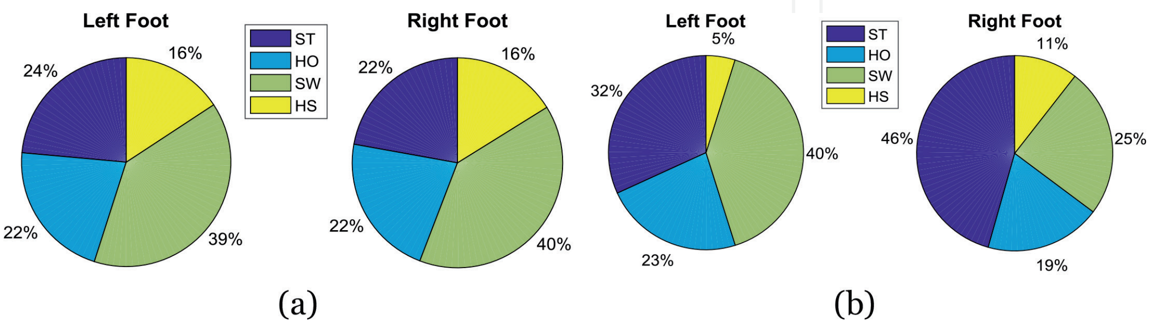

Figure 20.
Pie charts of the gait phases. (a) Healthy subject and (b) Hemiparesis patient.

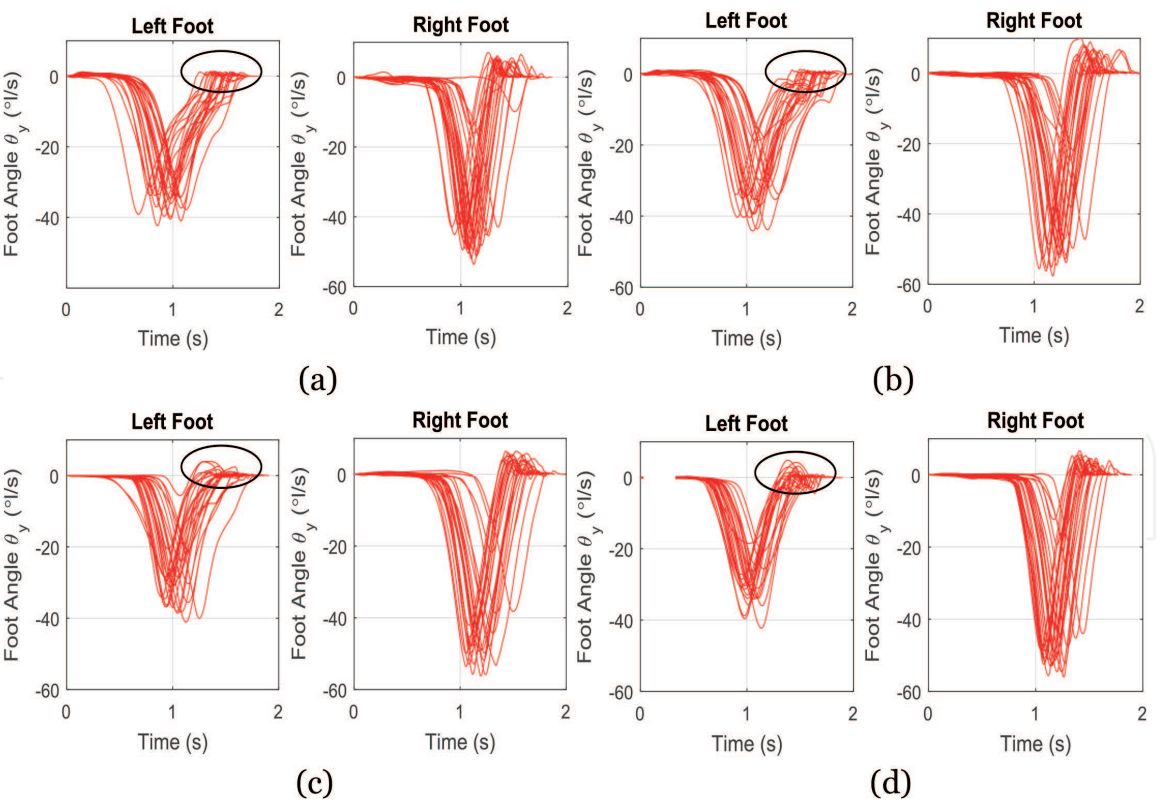

Figure 21.
Aligned extension-flexion angles of foot during rehabilitation. (a) First week, (b) Second week, (c) Third week and (d) Fourth week.

estimated foot angles of extension-flexion movement are shown in **Figure 21**, in which each region of maximum foot dorsiflexion angles is marked by an ellipse. For a better comparison, the angles over successive gait cycles are segmented and aligned along the time axis with the same starting point.

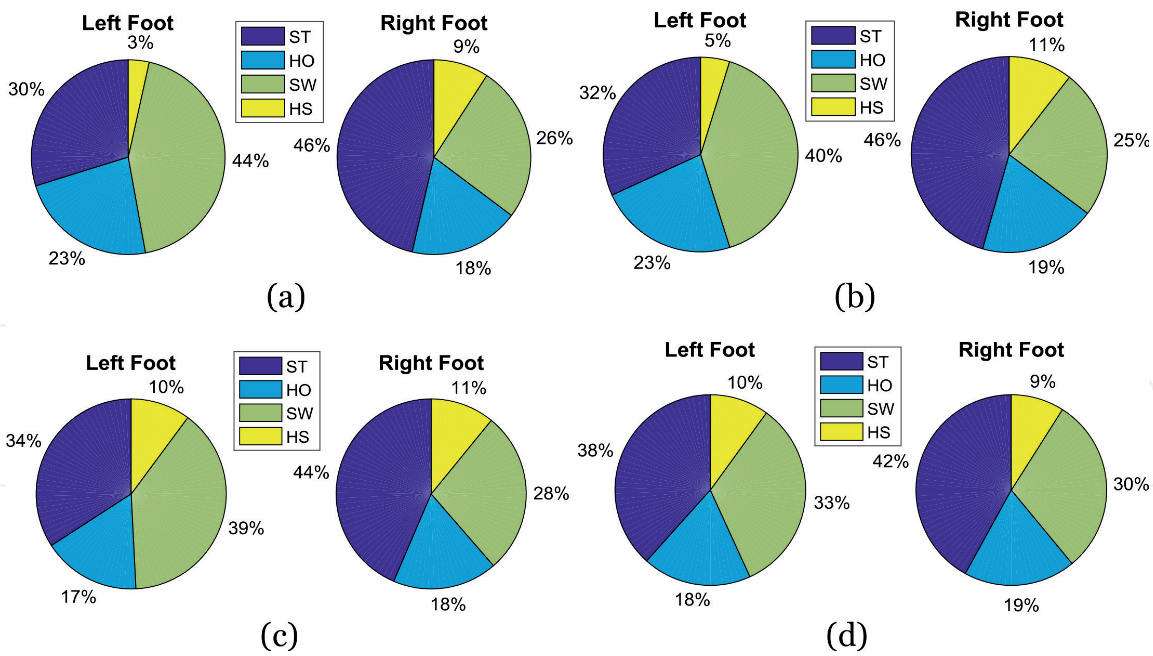

Figure 22.
Averaged percentages of gait phases during rehabilitation. (a) First week, (b) Second week, (c) Third week and (d) Fourth week.

As expected, the dorsiflexion range of the affected foot increased gradually as the treatment proceeded. If not, healthcare professionals may need to modify their treatment plans. Meanwhile, the gait symmetry of patient was also improved, as shown in **Figure 22** in terms of the percentages of the gait cycles spent in each concerned phase.

The conclusions drawn from **Figures 21** and **22** are consistent with that drawn in Sections 6.1 and 6.2. Based on the quantified spatiotemporal gait parameters that are provided by gyroscope-based foot-mounted gait analysis system, gait performance can be characterized to assess the rehabilitation process of patients with gait abnormalities, which is useful for deciding appropriate medical intervention.

7. Conclusions

Quantification of human gait via wearable inertial sensors has been attracting increasing interests in recent years, ranging from aiding pathologic diagnosis, choosing appropriate therapy, evaluating treatment efficacy, and assessing rehabilitation outcomes to monitoring gait degradation, predicting fall risks, and preventing elderly falls. This chapter demonstrated that gait analysis system constructed of foot-mounted MEMS gyroscopes could provide a promising way for estimating spatiotemporal gait parameters and has various potential uses in future research and clinical applications. Such systems are not only convenient for clinical diagnosis and treatment use but also can continuously monitor gait changes in nonclinical settings, thus providing seamless gait analysis from clinical to real-world settings.

However, although wearable technologies are regarded as solutions to create a more effective, convenient, and economical gait analysis technology, the potential of gait analysis has not been fully exploited thus far. There is still a great deal to do for its pervasive use. In future work, more gait parameters will be closely examined in the spatiotemporal domain, to conduct a thorough examination of person's pathological gait. Furthermore, reasonable indexes will be explored to evaluate the gait performance as fully as possible, and some nonlinear analysis techniques will be utilized to provide insight into the neuromuscular control processes that govern human locomotion.

Acknowledgements

This work was jointly supported by the China Postdoctoral Science Foundation no. 2017M621131, National Natural Science Foundation of China no. 61473058, and Fundamental Research Funds for the Central Universities no. DUT18RC(4)036 and DUT16RC(3)015.

Author details

Hongyu Zhao[1,2*], Sen Qiu[2], Zhelong Wang[2], Ning Yang[2], Jie Li[2] and Jianjun Wang[3]

1 Key Laboratory of Intelligent Control and Optimization for Industrial Equipment of Ministry of Education, Dalian University of Technology, Dalian, China

2 School of Control Science and Engineering, Dalian University of Technology, Dalian, China

3 Beijing Institute of Spacecraft System Engineering, Beijing, China

*Address all correspondence to: zhaohy@dlut.edu.cn

References

[1] Bioengineering B. BTS GAITLAB: Integrated Gait Analysis Systems [Internet]. 2019. Available from: https://www.btsbioengineering.com/products/bts-gaitlab-gait-analysis/ [Accessed: 22 March 2019]

[2] Physiotherapy S. Running and gait analysis [Internet]. 2019. Available from: https://southfieldsphysio.co.uk/index.php/services/running-gait-analysis [Accessed: 22 March 2019]

[3] Paramanandam V, Lizarraga KJ, Soh D, Algarni M, Rohani M, Fasano A. Unusual gait disorders: A phenomenological approach and classification. Expert Review of Neurotherapeutics. 2019;**19**(2):119-132

[4] Qiu S, Liu L, Zhao H, Wang Z, Jiang Y. MEMS inertial sensors based gait analysis for rehabilitation assessment via multi-sensor fusion. Micromachines. 2018;**9**(9):442

[5] Qiu S, Wang Z, Zhao H, Liu L, Jiang Y. Using body-worn sensors for preliminary rehabilitation assessment in stroke victims with gait impairment. IEEE Access. 2018;**6**:31249-31258

[6] Morris R, Hickey A, Del Din S, Godfrey A, Lord S, Rochester L. A model of free-living gait: A factor analysis in Parkinson's disease. Gait and Posture. 2017;**52**:68-71

[7] Zhao H, Wang Z, Qiu S, Ning Y, Shen Y. Examination of Gait Disorders in Hemiparesis Patients using Foot-Mounted Inertial Sensors. In: The 6th International Conference on Communications, Signal Processing, and Systems (CSPS '17); 14-16 July 2017; Harbin, China

[8] Zhao H, Wang Z, Qiu S, Shen Y, Wang J. IMU-based Gait Analysis for Rehabilitation Assessment of Patients with Gait Disorders. In: The 4th International Conference on Systems and Informatics (ICSAI '17); 11-13 November 2017; Hangzhou, China

[9] Therapy OP. Gait Analysis [Internet]. 2019. Available from: http://onpoint-pt.com/services/ [Accessed: 26 March 2019]

[10] Vicon. Motion Capture for Life Science [Internet]. 2019. Available from: https://www.vicon.com/motion-capture/life-sciences [Accessed: 26 March 2019]

[11] Chen S, Lach J, Lo B, Yang GZ. Towards pervasive gait analysis for medicine with wearable sensors: A systematic review. IEEE Journal of Biomedical and Health Informatics. 2016;**20**(6):1521-1537

[12] Qiu S, Wang Z, Zhao H, Liu L, Li J, Jiang Y, et al. Body sensor network based robust gait analysis: Toward clinical and at home use. IEEE Sensors Journal. 2019

[13] Zhao H, Wang Z, Shang H, Hu W, Gao Q. A time-controllable Allan variance method for MEMS IMU. Industrial Robot: An International Journal. 2013;**40**(2):111-120

[14] Choe N, Zhao H, Qiu S, So Y. A sensor-to-segment calibration method for motion capture system based on low cost MIMU. Measurement. 2019;**131**:490-500

[15] Zhao H, Wang Z, Gao Q, Hassan MM, Alelaiwi A. Smooth estimation of human foot motion for zero-velocity-update-aided inertial pedestrian navigation system. Sensor Review. 2015;**35**(4):389-400

[16] Qiu S, Wang Z, Zhao H, Qin K, Li Z, Hu H. Inertial/magnetic sensors based pedestrian dead reckoning by means of multi-sensor fusion. Information Fusion. 2018;**39**:108-119

[17] Zavala AV. Vascular and neuropathic foot. In: Cohen Sabban E, Puchulu F, Cusi K, editors. Dermatology and Diabetes. Cham: Springer; 2018. pp. 225-241

[18] Feliz R, Zalama E, Gómez-Bermejo JG. Pedestrian tracking using inertial sensors. Journal of Physical Agents. 2009;**3**(1):35-42

[19] Kotiadis D, Hermens HJ, Veltink PH. Inertial gait phase detection for control of a drop foot stimulator: Inertial sensing for gait phase detection. Medical Engineering and Physics. 2010;**32**(4):287-297

[20] Mannini A, Sabatini AM. Gait phase detection and discrimination between walking–jogging activities using hidden Markov models applied to foot motion data from a gyroscope. Gait and Posture. 2012;**36**(4):657-661

[21] Gouwanda D, Gopalai AA, Khoo BH. A low cost alternative to monitor human gait temporal parameters–wearable wireless gyroscope. IEEE Sensors Journal. 2016;**16**(24):9029-9035

[22] Sessoms PH. Step by step: A study of step length in able-bodied persons, race walkers, and persons with amputation. Dissertation Abstracts International: Section B: The Sciences and Engineering. 2009;**69**:6970

[23] Yamaguchi T, Hatanaka S, Hokkirigawa K. Effect of step length and walking speed on traction coefficient and slip between shoe sole and walkway. Tribology Online. 2008;**3**(2):59-64

[24] Miyazaki S. Long-term unrestrained measurement of stride length and walking velocity utilizing a piezoelectric gyroscope. IEEE Transactions on Biomedical Engineering. 1997;**44**(8):753-759

[25] Aminian K, Najafi B, Büla C, Leyvraz PF, Robert P. Spatio-temporal parameters of gait measured by an ambulatory system using miniature gyroscopes. Journal of Biomechanics. 2002;**35**(5):689-699

[26] Allseits E, Agrawal V, Lučarević J, Gailey R, Gaunaurd I, Bennett C. A practical step length algorithm using lower limb angular velocities. Journal of Biomechanics. 2018;**66**:137-144

[27] Jahn J, Batzer U, Seitz J, Patino-Studencka L, Boronat JG. Comparison and evaluation of acceleration based step length estimators for handheld devices. In: International Conference on Indoor Positioning and Indoor Navigation (IPIN '10); 15-17 September 2010; Zürich, Switzerland

[28] Zhao H, Wang Z, Qiu S, Shen Y, Zhang L, Tang K, et al. Heading drift reduction for foot-mounted inertial navigation system via multi-sensor fusion and dual-gait analysis. IEEE Sensors Journal. 2019

[29] Brand TJ, Phillips RE. Foot-to-foot range measurement as an aid to personal navigation. In: Proceedings of the 59th Annual Meeting of The Institute of Navigation and CIGTF 22nd Guidance Test Symposium; 23-25 June 2003; Albuquerque, NM, USA

[30] Qi Y, Boon SC, Erry G, Kay-Soon L, Rijil T. Estimation of spatial-temporal gait parameters using a low-cost ultrasonic motion analysis system. Sensors. 2014;**14**(8):15434-15457

[31] MEMSense. NANO IMU product specification and user's guide [Internet]. 2019. Available from: https://www.memsense.com/products/legacy/nano [Accessed: 30 March 2019]

[32] Analog Devices. ADIS16448 [Internet]. 2019. Available from: http://www.analog.com/en/products/sensors-mems/inertial-measurement-units/adis16448.html [Accessed: 15 October 2018]

[33] Wang Z, Zhao H, Qiu S, Gao Q. Stance-phase detection for ZUPT-aided foot-mounted pedestrian navigation system. IEEE/ASME Transactions on Mechatronics. 2015;**20**(6):3170-3181

[34] Bancroft J, Lachapelle G. Performance of Pedestrian Navigation Systems as a Function of Sensor Location. In: Proc NATO Symposium Navigation Sensors and Systems in GNSS Denied Environments; 8-9 October 2012; Izmir, Turkey

[35] Wang J, Wang Z, Zhao H, Qiu S, Li J. Using wearable sensors to capture human posture for lumbar movement in competitive swimming. IEEE Transactions on Human-Machine Systems. 2019;**49**(2):194-205

[36] Zhao H, Wang Z, Qiu S, Wang J, Xu F, Wang Z, et al. Adaptive gait detection based on foot-mounted inertial sensors and multi-sensor fusion. Information Fusion. 2019;**52**:157-166

[37] li J, Wang Z, Wang J, Zhao H, Qiu S, Yang N, et al. Inertial sensor-based analysis of equestrian sports between beginner and professional riders under different horse gaits. IEEE Transactions on Instrumentation and Measurement. 2018;**67**(11):2692-2704

[38] Taborri J, Palermo E, Rossi S, Cappa P. Gait partitioning methods: A systematic review. Sensors. 2016;**16**(1):20

[39] Fischer C, Sukumar PT, Hazas M. Tutorial: Implementing a pedestrian tracker using inertial sensors. IEEE Pervasive Computing. 2013;**12**(2):17-27

[40] Strömbäck P, Rantakokko J, Wirkander SL, Alexandersson M, Fors I, Skog I, et al. Foot-mounted inertial navigation and cooperative sensor fusion for indoor positioning. In: Proceedings of the International Technical Meeting of the Institute of Navigation (ITM '10); 25-27 January 2010; San Diego, CA

[41] Abdulrahim K, Hide C, Moore H, Hill C. Integrating low cost IMU with building heading in indoor pedestrian navigation. Journal of Global Positioning Systems. 2011;**10**(1):30-38

[42] Skog I, Händel P, Nilsson JO, Rantakokko J. Zero-velocity detection—An algorithm evaluation. IEEE Transactions on Biomedical Engineering. 2010;**57**(11):2657-2666

[43] Yun XP, Calusdian J, Bachmann ER, McGhee RB. Estimation of human foot motion during normal walking using inertial and magnetic sensor measurements. IEEE Transactions on Instrumentation and Measurement. 2012;**61**(7):2059-2072

[44] Godha S, Lachapelle G. Foot mounted inertial system for pedestrian navigation. Measurement Science and Technology. 2008;**19**(7):1-9

[45] Abaid N, Cappa P, Palermo E, Petrarca M, Porfiri M. Gait detection in children with and without hemiplegia using single-axis wearable gyroscopes. PLoS ONE. 2013;**8**(9):e73152

[46] Taborri J, Scalona E, Palermo E, Rossi S, Cappa P. Validation of inter-subject training for hidden Markov models applied to gait phase detection in children with cerebral palsy. Sensors. 2015;**15**(9):24514-24529

[47] Guenterberg E, Yang AY, Ghasemzadeh H, Jafari R, Bajcsy R, Sastry SS. A method for extracting temporal parameters based on hidden Markov models in body sensor networks with inertial sensors. IEEE Transactions on Information Technology in Biomedicine. 2009;**13**(6):1019-1030

[48] Evans RL, Arvind D. Detection of gait phases using orient specks for mobile clinical gait analysis. In: The 11th

International Conference on Wearable and Implantable Body Sensor Networks; 16-19 June 2014; Zurich, Switzerland

[49] Ogiela MR, Jain LC. Computational Intelligence Paradigms in Advanced Pattern Classification. Berlin Heidelberg: Springer; 2012

[50] Hecht-Nielsen R. Theory of the backpropagation neural network. In: Wechsler H, editor. Neural Networks for Perception. Academic Press; 1992. pp. 65-93. https://www.sciencedirect.com/book/9780127412528/neural-networks-for-perception#book-description

[51] Zhao H, Wang Z, Qiu S, Li J, Gao F, Wang J. Evaluation of inertial sensor configurations for wearable gait analysis systems. In: The 20th IEEE/ACIS International Conference on Software Engineering, Artificial Intelligence, Networking and Parallel/Distributed Computing (SNPD '19); 8-10 July 2019; Toyama, Japan

[52] Zhao H, Shang H, Wang Z, Jiang M. Comparison of initial alignment methods for SINS. In: World Congress on Intelligent Control and Automation (WCICA '11); 21-25 June 2011; Taipei, Taiwan